We are IntechOpen, the world's leading publisher of Open Access books Built by scientists, for scientists

4,800
Open access books available

122,000
International authors and editors

135M
Downloads

Our authors are among the

154
Countries delivered to

TOP 1%
most cited scientists

12.2%
Contributors from top 500 universities

CLARIVATE ANALYTICS BOOK CITATION INDEX INDEXED

WEB OF SCIENCE™

Selection of our books indexed in the Book Citation Index in Web of Science™ Core Collection (BKCI)

Interested in publishing with us?
Contact book.department@intechopen.com

Numbers displayed above are based on latest data collected.
For more information visit www.intechopen.com

12

Ultrasonic-Based Distance Measurement Through Discrete Extended Kalman Filter

Leopoldo Angrisani, Aldo Baccigalupi and Rosario Schiano Lo Moriello
Università degli Studi di Napoli
Italy

1. Introduction

Ultrasonic-based measurements are extensively used both in research and production field, spanning in endless applications: environment sensing of autonomous mobile robots, high definition imaging of biomedical devices, precise location of micro-flaws in materials, accurate estimation of the level of flammable fluids or dangerous rivers, and so on. The reason of this success mainly relies upon the opportunity offered by ultrasonics of conceiving rather simple methods or building up relatively cheap meters, characterized by satisfactory accuracy, reduced measurement time, and, above all, high level of intrinsic safety.

The measuring principle of most methods is the estimation of the time-of-flight (TOF) of an ultrasonic burst (high-frequency sinusoidal pulse train) generated by a proper transducer; i.e. the time elapsing between the firing up of the transducer and the detection of the echo originated by any discontinuity or reflector in the propagation medium. The desired information, x, concerning distance (the object of unknown distance acts like a reflector), or level (the surface of the fluid of unknown level gives rise to a discontinuity), or integrity (any crack in the structure under test disturbs medium continuity) is then gained through a very common and straightforward expression:

$$x = \frac{c \cdot t}{2} \tag{1}$$

where c is the propagation velocity of the ultrasonic burst, and t is the TOF estimate.

Two sequential steps generally characterize TOF-based measurements. The first step provides for the digitization of the received ultrasonic signal through a data acquisition system (DAS), while in the second one a suitable digital signal-processing (DSP) algorithm is applied to the acquired samples for the desired TOF to be estimated. Major sources of inaccuracy can be found in additive noise affecting the acquired ultrasonic signal, shape distortion of the received echo, and dependence on temperature of the propagation velocity.

To face noise problems, DSP algorithms implementing the cross-correlation estimator (CCE), or matched filter, have been proposed. In the presence of additive, zero mean, white Gaussian noise, the CCE is, in fact, proven to be optimal according to maximum likelihood criterion, provided that no shape distortion of the received echo occurs. When the last assumption is violated, TOF estimates become significantly biased, and the amount of bias can be much greater than the experimental standard deviation.

Source: Kalman Filter: Recent Advances and Applications, Book edited by: Victor M. Moreno and Alberto Pigazo,
ISBN 978-953-307-000-1, pp. 584, April 2009, I-Tech, Vienna, Austria

To mitigate distortion effects, generalized versions of the conventional CCE have been defined and implemented. More specifically, parametric models of the echo envelope, which produce a sort of correlation function, are built concurrently with the process of TOF estimation. Benefits in bias reduction are, however, gained to the detriment of noise sensitivity and, above all, computational burden.
Concerning the influence of temperature in TOF-based measurements, the most popular method for avoiding accuracy loss is to duly check its value by an external sensor. Straightforward relations, in fact, apply for establishing the actual propagation velocity according to the current value of the temperature.
An original use of *discrete extended Kalman filter* (DEKF) is presented in the following to face the aforementioned problems. The novelty of the method mainly relies upon its capability of jointly estimating the whole set of parameters (A_0, α, T, and τ) that characterize the well-known model of echo envelope, $A(t)$:

$$A(t) = A_0\left(\frac{t-\tau}{T}\right)^{\alpha}\exp\left(\frac{t-\tau}{T}\right) \tag{2}$$

A_0 accounts for echo amplitude, α and T are peculiar to the specific ultrasonic transducer, and τ is the desired TOF [4]-[6]. The main advantage of the new approach is that TOF estimation inherently accounts for distortions the ultrasonic echo eventually undergoes, with a consequent positive effect on bias reduction. An original use of the DEKF allows the desired joint estimation of the aforementioned four parameters to be pursued. Specifically, after modeling the echo envelope as a stochastic process whose state is identified by the considered parameters, the DEKF provides a robust and reliable solution of the non-linear equation system involved.

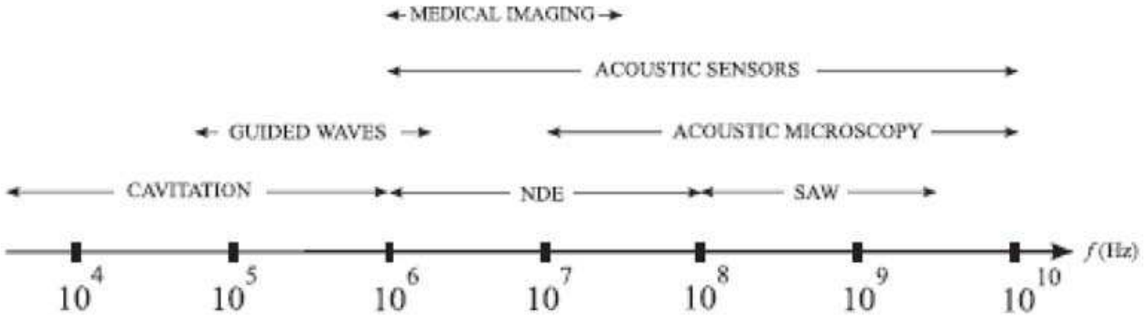

Fig. 1. Common frequency ranges for various ultrasonic processes.

2. Ultrasonic-based distance measurement: state of the art

The contactless and cheap measurement of distances in the range of a few millimiters to a few meters is a strategic task in several fields [1]-[3]. Although several solutions providing good accuracy can be conceived, for example optical solutions which are based on lasers or position sensitive devices, such solutions are usually rather expensive. In addition, in several cases the use of lasers or other high-power systems cannot be accepted in hazardous environments or when low energy devices are prescribed [4]. In these cases low-power ultrasonic sensors are a cost-effective solution, especially when low-frequency devices (30-50

kHz) are used [5]-[7]. What are ultrasounds? Like the visible spectrum, the audio spectrum corresponds to the standard human receptor response function and covers a frequency range from 20 Hz to 20 kHz, although, with age, the upper limit is reduced significantly. For both light and sound, the "human band" is only a tiny slice of the total available bandwidth. In each case the full bandwidth can be described by a complete and unique theory, that of electromagnetic waves for optics and the theory of stress waves in material media for acoustics. Ultrasonics is defined as that band above 20 kHz. It continues up into the MHz range and finally, at around 1 GHz, goes over into what is conventionally called the *hypersonic* regime. The full spectrum is shown in Fig.1, where typical ranges for the phenomena of interest are indicated. Most of the applications of interest take place in the range of 1 to 100 MHz, corresponding to wavelengths in a typical solid of approximately 1 mm to 10 μm, where an average sound velocity is about 5000 m/s. In water—the most widely used liquid—the sound velocity is about 1500 m/s, with wavelengths of the order of 3 mm to 30 μm for the above frequency range.

An advantage of measuring methods exploiting ultrasonic waves is that they enable the direct accomplishment of a digital measurement without the need for conversion of an analog signal to a digital one by an analog-to digital converter (ADC). In most applications, either the velocity of the ultrasonic wave or the time of flight of a wave over the measured distance is utilized. From a technological point of view, another advantage is that the propagation velocity of ultrasonic waves is many orders lower than that of electromagnetic waves. Because of this, less stringent demands are required on the transducers and associated electronic circuits. On the other hand, the use of ultrasonic waves has certain drawbacks too, in particular the large dependence of their propagation velocity on the parameters of the propagation medium, and their high attenuation and scattering, especially in air.

These circumstances determine the boundaries for the full exploitation of ultrasonic measuring methods. In the first instance, they are limited to relatively small distances, compared with methods employing electromagnetic radiation. In case where more accurate measurements are required, ultrasonic techniques become more complicated due to the need to compensate for the effects of fluctuations of the parameters of the propagation medium. In the following, some general methods are described which are most often used for in-air distance measurement.

2.1 Classification of measurement methods

Measuring methods can roughly be divided into two fundamental groups. One of them uses a continuous (harmonic, periodic) wave motion, the other one uses discontinuous (pulsed) waves. The case of harmonic ultrasonic waves is commonly used to evaluate the phase shift between the transmitted and the received signals. The phase change is dependent on the measured quantity, e.g. a distance, in an unchanged and stationary medium, on the composition the (fluid) medium at a stationary distance between the transducers, and on the medium flow rate, temperature, etc. Therefore, these methods can be included in the group of methods which use phase modulation.

In the case of measurements involving a pulsed ultrasonic wave, the duration of the pulse propagation, from the transmitter (pulse generator) to the receiver (pulse front detector), is usually evaluated. The duration of the pulse propagation depends on the transmitter-receiver distance, as well as on the properties (and the motion) of the intervening medium.

It is worth noting that it is possible for the same transducer to act as transmitter and receiver, thus allowing a reduction of complexity of the meter. Generally this method can be classified among those using time-pulse modulation. In the case of the detection of a reflected pulsed ultrasonic wave from an object, the method is analogous to the radiolocation method. Both methods have advantages and drawbacks of their own.
It is worth noting that, although accurate, the phase determination is insufficient for the evaluation of the pulse propagation because the result has a periodicity of one carrier wavelength. This way, in the following, measuring methods using pulsed ultrasonic waves will only be analyzed in details; in particular, the most interesting solutions, in order of increasing measurement reliability, are presented.

2.2 Measurement method based on threshold detection

As stated above, pulse methods evaluate the time of propagation (i.e. the time of flight, TOF) of an ultrasonic pulse wave from a transmitted to a receiver. For the case of distance measurement, a typical example of a digital evaluation of the TOF [8] is illustrated in Fig.2.
At the start of a measurement, a pulse generator excites a voltage pulse, V_i. This is converted in the transmitter to an ultrasonic pulse which propagates towards the receiver at a velocity c. After the front edge of the pulse wave falls on the active surface of the receiver, a voltage, V_a, appears at the amplifier output. When the amplitude of the received signal overcome a fixed threshold the echo is assumed to be detected, and the time measuring pulse, V_p is stopped. The conversion of the pulse propagation time into a number N_x is then carried out by a circuit depicted in the lower part of Fig.2.a; at its input there is a bistable circuit whose output is set to the active (logical one) state.

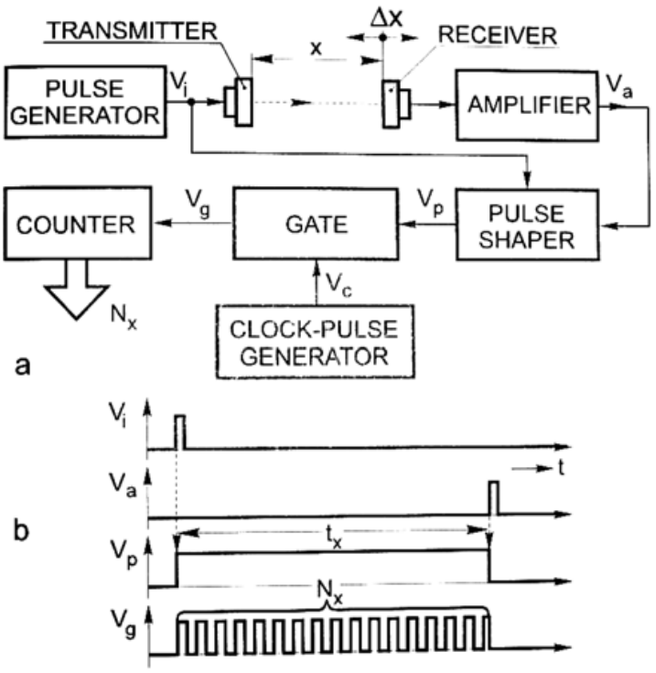

Fig. 2. Measurement of distance through threshold-based method.

This results in the opening of the gate through which pulses, V_c, begin to pass from the clock (time mark) generator to a reversible counter. After arrival of the pulse V_a, the bistable

returns to its initial (zero) state and the measurement is over. On the counter display, a number N_x appears which corresponds to the measured distance. The process described is illustrated in the time diagrams of Fig.2.b.
The measured distance, x, can be expressed through the propagation time, TOF, of the ultrasonic wave as

$$x = cTOF \quad or \quad x = \frac{c}{2}TOF \tag{3}$$

according to the type (direct or reflected) of performed measurement. At the same time, it is also true that N_x=fTOF, where f stands for the clock fundamental frequency. By considering the inherent error of the time-to-digital conversion (i.e. the quantization error), it can be written

$$x = \left(\frac{c}{f}\right)\left(N_x \pm 1\right) \tag{4}$$

In order to read the distance in a straightforward way in length units, its value should be expressed in decimal order of tens. In order to lower the discretization error, the working frequency of the clock is chosen sufficiently high (as a rule, tens of MHz are used). As an example, if 20 °C is the environmental temperature in the working space, the frequency can be 34.37 MHz. On measuring a distance of x=1 m, there is a reading N_x of 100000±1 on the counter display; the resolution is then 10 μm.
The threshold method proves itself very easy and simple to realize on actual sensor. Its main drawback is the uncertainty associated to the instant of detection of the received signal. As for all the similar threshold method, the echo receiver suffers from noise sensitivity: in fact, spike superimposed to the useful signal can give rise to spurious identification of the TOF. Finally, the threshold does not identify the right onset of the signal; this way, the obtained measurements are unavoidably biased. The problem is makes worse in the presence of signal shape distortion.

2.3 Measurement methods based on cross-correlation estimator

Measurement method based only on cross-correlation estimator

When higher accuracy are required, methods based on cross correlation estimator are suggested [9]. Measurement of the time of flight can be considered in the general framework of time delay estimation. The transducer generates a signal, $s(t)$, that propagates to the target and is reflected back, being detected after a delay D. The TOF measurement system has to determine this time interval.
The propagating medium introduces attenuation that increases with frequency, and can distort the reflected wave. However, if the pulse is narrow-band, attenuation by a constant coefficient α can be assumed for the delayed echo, so that one can express it in the form $\alpha s(t\text{-}D)$. In practice, these hypotheses are satisfied only approximately. Furthermore, external disturbances such as turbulence and vibrations may affect the signal waveform, and quantization noise is introduced by the conversion process. The measurement system acquires the two digital sequences $x_T(nT)$ and $x_E(nT)$ representing the transmitted and echo signals, respectively, that can be written in the form

$$\begin{aligned} x_T(nT) &= s(nT) + v(nT) \\ x_E(nT) &= \alpha s(nT) + n(nT) \end{aligned} \tag{5}$$

where T is the sampling interval, while $v(nT)$ and $n(nT)$ take into account the discrepancies from the ideal model and can be considered as zero mean uncorrelated random processes. It is worth noting that the transmitted signal, $x_T(nT)$, is taken as reference, and the cross-correlation function is always evaluated through this signal. The cross-correlation of the two sequences is given by:

$$C(kT) = \sum_{n=-\infty}^{n=\infty} x_T(nT) x_E(nT + kT) \tag{6}$$

According to the hypotheses given above on $v(nT)$ and $n(nT)$, the statistical expectation of this sequence is:

$$E[C(kT)] = \alpha C_{ss}(\tau - D)\big|_{\tau = kT} \tag{7}$$

where $C_{SS}(\tau)$ is the auto-correlation function of the continuous signal $s(t)$. Therefore, if k_D is the index of the peak of $E[C(kT)]$, it can be stated that $D = k_D T$ when the delay is an integer multiple of the sampling interval, and $D = (k_D + \delta)T$, with $|\delta| < 0.5$, otherwise. In practice, the delay can be estimated by finding the maximum of the cross-correlation function (6). A typical expression of the ultrasonic signal is:

$$s(t) = a(t)\sin(2\pi f_0 t + \phi) \tag{8}$$

where f_0 is the transducer resonant frequency, and the pulse $a(t)$ represents the signal envelope and has finite duration. For this class of signals, the following expression holds:

$$C_{ss}(\tau) = C_{aa}(\tau)\frac{1}{2}\cos(2\pi f_0 \tau) \tag{9}$$

$C_{aa}(\tau)$ stands for the auto-correlation function of the signal envelope $a(t)$. This suggests the possibility of estimating the delay from the cross-correlation function, $C_{aa}(\tau)$, of signal envelopes, with the advantage that improved resolution can be expected, since the sinusoidal term is no longer present. Depending on the distance to be measured, the TOF can be quite large, resulting in very long data sequence if the echo signal is sampled continuously. However, since $s(t)$ in (6) has finite duration, an interval occurs between the transmitted and echo pulses, where the only relevant information is the count of samples falling within.

If the onset of the echo can be detected by some simple experiment, the sequence of echo samples, $x_E(nT)$, can be much shorter. In fact, it suffices that its length N is equal to that of the sampled transmission sequence $x_T(nT)$, the only requirements being that the time interval NT is longer than the duration of $s(t)$ and that the echo is entirely contained in the sequence. If this is the case, the TOF is determined by algebraically adding the delay estimate provided by the algorithm to the number of samples that were counted before the

acquisition of the echo sequence. The main advantage lies in the reduced computations involved in processing shorter sequences.

The first step of the algorithm is to recover from the sequences $x_T(nT)$ and $x_E(nT)$ their sampled envelopes, that will be indicated as $y_T(nT)$ and $y_E(nT)$, respectively. It is apparent from (4) that the transducer output can be interpreted as an amplitude modulated signal having carrier frequency f_0; this suggests the use of demodulation. After analyzing and trying different methods, an usual choice is to realize in digital form a square law envelope detector. This is a simple kind of demodulator that does not require accurately determining the carrier frequency f_0, thus avoiding the need for a specific setup of the system if different ultrasonic transducers must be used. After demodulated, the cross-correlation function of transmitted and received envelope is evaluated according to:

$$C(kKT) = \sum_{n=0}^{(N/K)-1} y_T(nKT)\, y_E(nKT + kKT)$$
$$k = -\frac{N}{K} + 1, \ldots, \frac{N}{K} - 1 \tag{10}$$

where K is a suitable decimation factor needed to reduce the number of acquired samples. If the delay D has a fractional component (i.e., $\delta \neq 0$), the peak of the corresponding continuous correlation function does not coincide with the position of the sample of index k_D.

The fractional index δ can be determined from the samples of $C(kKT)$ through an interpolation formula. Although its analytical expression can be given, in most practical cases the relationship is unlikely to be satisfied exactly. Therefore, it was decided to avoid this complication and rely instead on an approximate interpolation formula. Given the samples with index k_D, $k_D - 1$ and $k_D + 1$, a simple second-order polynomial approximation of $C(t)$ yields a parabola, and the fractional index δ is obtained as the abscyssa of its vertex. Dropping for simplicity the term KT from the argument of $C(kKT)$, it can be written:

$$\delta = \frac{C(k_D + 1) - C(k_D - 1)}{2[2C(k_D) - C(k_D - 1) - C(k_D + 1)]} \tag{11}$$

Results provided by the cross-correlation estimator have been reported for a set of experiments carried out in the presence of different transducer-to-target distances, with reference distance measurements being obtained by laser interferometry. Experimental data are reported in Tab.1. As suggested by the authors of the paper, all distances are measured with respect to a common reference point; that represents zero distance; the TOF related to this point is always subtracted from subsequent measurements. This enables compensation for a number of possible factors that introduce offsets, such as time delays between the digitizer trigger and the actual start of the transmit pulse, in the evaluation of the origin for measuring distance.

Measurement method based on combined use of cross-correlation estimator and phase shift evaluation

The phase shift method, in addition to the correlation method, has been suggested in order to enhance the accuracy [10]. It relies on the property that, for a sampled cosine signal, one can determine the phase shift from the origin by computing the coefficient of the discrete

Fourier transform (DFT) corresponding to the frequency of this cosine wave. This calculation is more or less complex, depending mainly on the relation between the cosine frequency and the sampling rate.

Reference (mm)	Measured Distances (points)	Measured Distances (mm)	Difference (mm)
0	0	0	—
100.0	146.0	100.7	+0.7
203.5	296.8	204.8	+1.3
306.0	443.7	306.1	+0.1
407.2	589.1	406.5	−0.7
503.8	729.5	503.4	−0.4
600.8	869.8	600.2	−0.6
698.8	1013.6	699.4	+0.6
799.4	1159.1	799.8	+0.4
898.9	1303.5	899.4	+0.5
998.7	1448.7	999.6	+0.9
1101.1	1598.1	1102.7	+1.6
1200.2	1736.9	1198.5	−1.7

Tab. 1. TOF-based distance measurement

If the sampling time is strictly synchronized with the transmission signal, the *phase shift* between transmission and reception *carriers* can be evaluated by computing the phase shift of the received signal from the sampling time reference. A good choice of the sampling rate can simplify the calculation of the corresponding DFT coefficient.
The final TOF resulting from using both methods simultaneously is

$$TOF = \frac{\left(k_D + \frac{\alpha}{2\pi}\right)}{f_0} \tag{12}$$

where k_D is the integer number of carrier wavelengths inferred from the correlation result, α the phase shift, and f_0 the carrier frequency. It is worth noting that, although accurate, the phase determination is insufficient for the evaluation of the TOF because the result has a periodicity of one carrier wavelength. Among the positions determined by phase computation, the one which is nearest to the maximum of the cross-correlation parabolic approximation previously determined, is the final value of the measured TOF.
From an operative point of view, the first step of the method consists of applying the aforementioned cross-correlation approach (upper evaluation path in Fig.3). The second path calculates the phase difference between the transmitted and received waves. This value can be computed by using the DFT coefficient of the acquired sample *r(n)* corresponding to the carrier frequency (the transmitted signal is replaced by the synchronous sampling clock). The proper choice of the sampling rate simplifies the calculation of the phase difference. The computed phase-shift has an accuracy mainly limited by the amplitude accuracy of the

samples and thus the resolution of the A/D converter used for digitization. Moreover, simulations has shown that the phase evaluation is significantly less affected by the additive white noise than the cross-correlation peak determination.

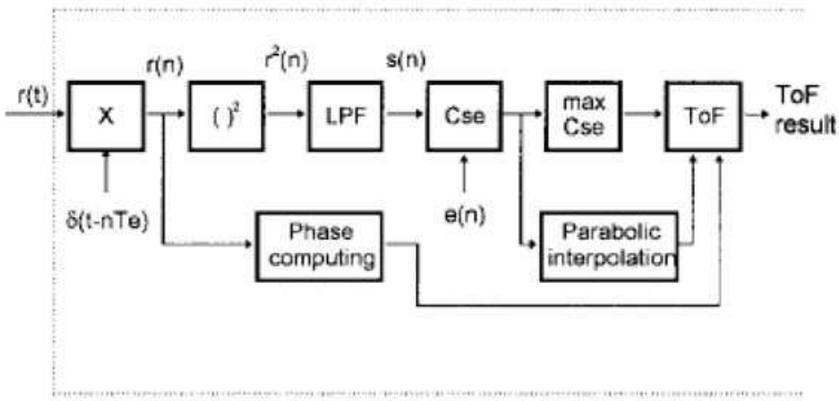

Fig. 3. Measurement algorithm combining cross-correlation estimator and phase shift methods

Results presented by the authors highlight the strong improvement due to the combination of the two methods (Fig.4). For each trial reported in abscissa, gives the distance (expressed in number of carrier wavelengths, λ) computed successively by the correlation-only method (Fig.4.a) and the combined (correlation plus phase; λ = 9 mm) method (Fig.4.b).

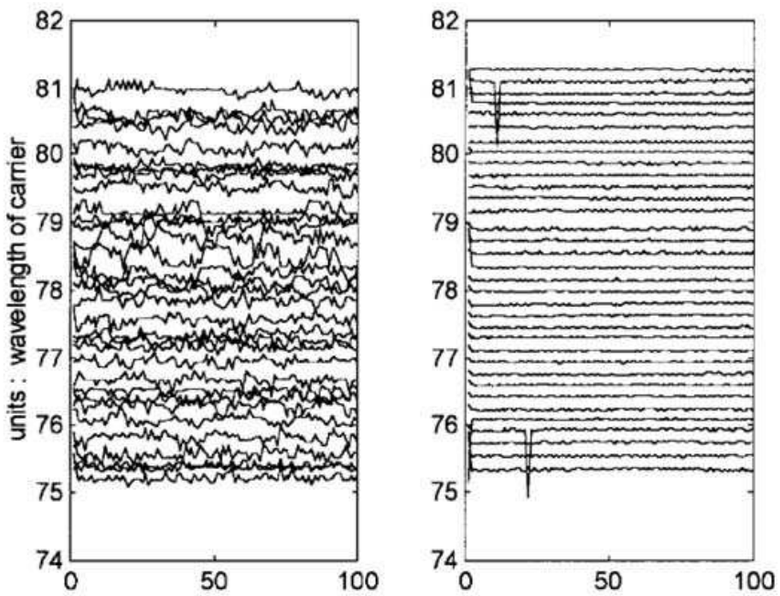

Fig. 4. Measurement results (a) from correlation method and (b) from correlation plus phase method.

Moreover, Fig.5 shows the difference in distance versus the position, of each result for both methods, with reference to the linear regression of the mean results (evaluated upon 100 independent measurements for each distance value) obtained by the combined method ("phase results"). The continuous curves (combined method is the upper curve) are the

fluctuations of the mean, the vertical segments are the total excursion of the results at each position, and the dots represent the standard deviations. The pseudoperiodicity of about 4.8 mm, about half of a wavelength at the sampling frequency, of the results obtained by the correlation-only method is explained by a residual effect of the squaring in the computing algorithm due to an imperfect filtering. The computation of the mean standard deviation averaged over all the positions gives for the combined method a value of 0.07 mm.

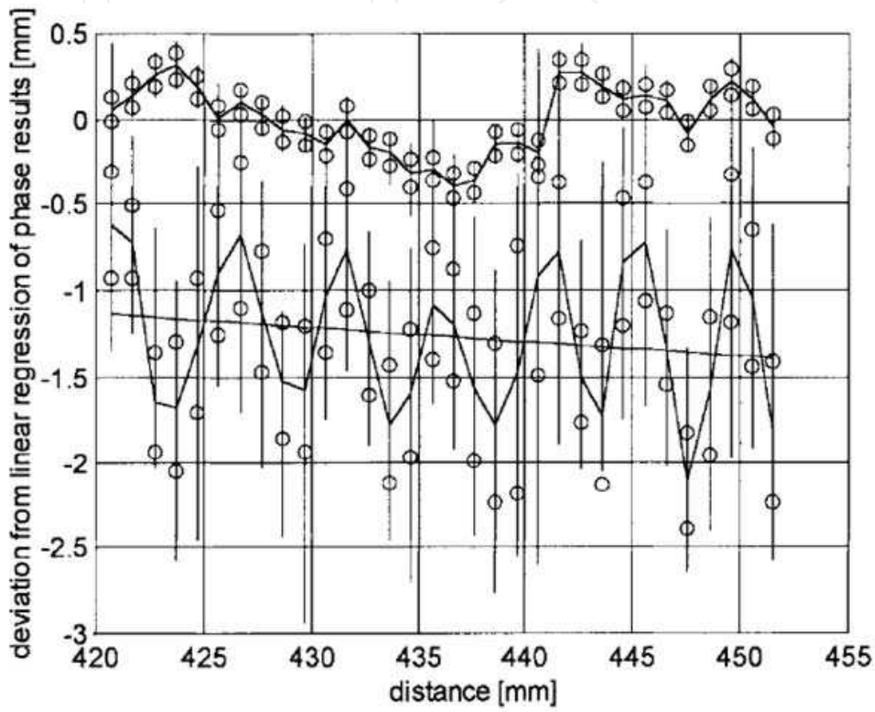

Fig. 5. Distance deviations from linear regression of the mean of results obtained by the combined ("phase") method.

Drawbacks

Despite of the its simplicity, cross-correlation estimation suffers from a dramatic drawback. As aforementioned, it aims at identifying the maximum value of the cross-correlation between the return signal and a properly chosen reference signal [11]. The cross-correlation estimator, or matched filter (MF) is proven to be optimal according to the maximum likelihood (ML) criterion for signals embedded in additive white Gaussian noise with zero mean, provided that time-delayed, amplitude-scaled, nonoverlapping replicas of the reference signal are actually contained in the return signal [12].

When the assumption that the shapes of the received echoes do not change is violated, the estimator is no longer optimal. Usually, the efficiency of non-matched filters is taken as the peak signal-to-noise ratio (SNR) from the non-matched filter divided by the peak SNR from the MF [13]. Actually, the consequence of shape distortions is that the cross-correlation estimator becomes biased, and the amount of bias can be much greater than the standard deviation of the TOF estimates [14]. Echo shape distortions occur in consequence of many factors. The geometrical properties of the insonified reflector play a major role in modifying the echo shape; the position and orientation of the object relative to the ultrasonic sensor, the

propagation path, and some environmental factors such as temperature and humidity also have an influence. The ability of modeling the echo shape is thus a requisite that correlation-based ultrasonic sensor systems should possess in order to accomplish object ranging and identification. To overcome the problem of the polarization, some authors suggested the possibility of simultaneously estimating the envelope of a narrowband signal embedded in additive noise and its time delay in the case that the a priori information about the shape of the signal is minimal.

2.4 Measurement method based on generalized cross-correlation estimator

As stated above, most methods facing the problem of the polarization involve techniques for joint distance measurement and model-based estimation of the echo shape. One of the most successful solution is a method based on a truncated series expansion of the echo envelope by a set of Laguerre basis functions [20]. Laguerre functions are widely used in the field of system identification to approximate the impulse response of a causal linear time-invariant stable system [15]. They are exploited in the context of simultaneous system identification and TOF estimation. The outputs of the Laguerre filter bank that computes the running Laguerre transform are used to build a generalized correlation function. The envelope of the echo from an unknown object is represented by the set of expansion coefficients, e.g., the Laguerre spectrum, which we need to estimate together with the unknown TOF. Differently from other generalized cross-correlation techniques [14], a reference signal is not required (unconstrained signal modeling); the only a priori information available to the receiver that may be used to attenuate its noise sensitivity is given by some smoothness conditions regarding the value of the unknown reference signal and of its first time derivative at the signal onset (constrained signal modeling). These signal constraints are motivated by empirical observations of typical ultrasonic sensor signals in a variety of experimental conditions. Let us suppose that the signal observation model is of the form:

$$r(t) = s(t-\tau) + n(t) \tag{13}$$

Here, τ is the TOF to be estimated. $s(t)$ is assumed to be a narrowband signal, with center frequency f_0 (the ultrasonic carrier frequency) and bandwidth $B \ll f_0$. Accordingly, $s(t)$ can be represented in terms of its complex envelope $\tilde{s}(t)$ as follows:

$$s(t) = \Re\{\tilde{s}(t)\exp(j2\pi f_0 t)\} \tag{14}$$

$\Re\{\cdot\}$ indicates the real part of its argument. By definition, the complex envelope of a narrowband signal is a low-pass, complex-valued signal with bandwidth B. Its magnitude $\mu_s(t)$ is the envelope of $s(t)$. The task to be accomplished concerns the joint estimation of $\mu_s(t)$ and τ, in the case that the additive noise $n(t)$ is white Gaussian, having zero mean and power spectral density $N_o/2$.

A typical expression of the envelope $A(t)$ is given in terms of functions

$$A(t) = \left(\frac{t}{T}\right)^m \exp\left(-\frac{t}{T}\right) U(t) \tag{15}$$

with $1 < m < 3$ (damped exponential model with exponent m). T is a transducer-dependent time constant and $U(t)$ is the unit step function.

The Laguerre functions are obtained by orthonormalizing the functions $t^i \exp(-at)$, $i \in N$, $a>0$:

$$l_i(t,a) = \sqrt{2a}\exp(-at)\sum_{j=0}^{i} C_j^i \frac{(-2at)^j}{j!} \tag{16}$$

where C_j^i is the binomial coefficient [16], and the parameter a, also called the time scaling factor of the Laguerre series, is related to the pole position of the Laplace transforms of the Laguerre functions. Laguerre functions act the same role of the sinusoidal functions in the Fourier transform; in fact, the nature of typical signals produced by in-air ultrasonic sensors is strongly in support of using a set of Laguerre functions which decay exponentially to zero at a controllable rate for their representation:

$$A(t) \stackrel{\Delta}{=} \sum_{i=0}^{Q} c_i(a) l_i(t,a) \tag{17}$$

Q stands for the model order, and $c_i(a)$ is the i-th coefficient of the Laguerre spectrum. Along with the time-of-flight, t, they are unknown and needed to be estimated from noisy observations of the signal $s(t)$. It should be noted that the time scaling factor a is critical for achieving accurate approximations of a given signal by a truncated series of Laguerre functions. In fact, for any value of the time scaling factor, the Laguerre coefficients are computed by minimizing the approximation error in the least-square sense. Optimal values of a are thus to be computed by searching for the global minimum of the squared error surface of these approximations; the numerical techniques that are available for this purpose are expensive in computational terms [17]. An optimal choice of the time scaling factor also should provide a minimum of significant coefficients of the Laguerre spectrum [18].

In spite that the theory presented concerns Laguerre functions and analog signals, it can take advantage of using sampled signals to implement an equivalent discrete-time version of the correlation receivers. The block diagram of a correlation receiver of order M is depicted in Fig.6. The magnitude $\mu_r(kt)$ of the complex envelope of the return signal is computed by means of the Hilbert transform method [19].

The output of the receiver are the M-th order discrete-time generalized correlation function (GCF) and constraining function (CF). TOF is identified by means of both the functions: in particular, GCF is employed to achieve a rough TOF estimate. One local minimum of the CF then occurs at the same time instant when the GCF takes its global peak, thus allowing TOF to be reliably located (Fig.7).

The performance of the GCF method has been assessed through computer simulations and experimental results using a simple US sensor system. At high SNRs the proposed constrained correlation receiver performs better than conventional matched filters if echo shape distortions not properly accounted for in the selection of the reference signal of the matched filters are present; in fact, such distortions are known to produce biased TOF estimates. The proposed receiver trades the bias removal for the increased noise sensitivity at low SNRs (Fig.8).

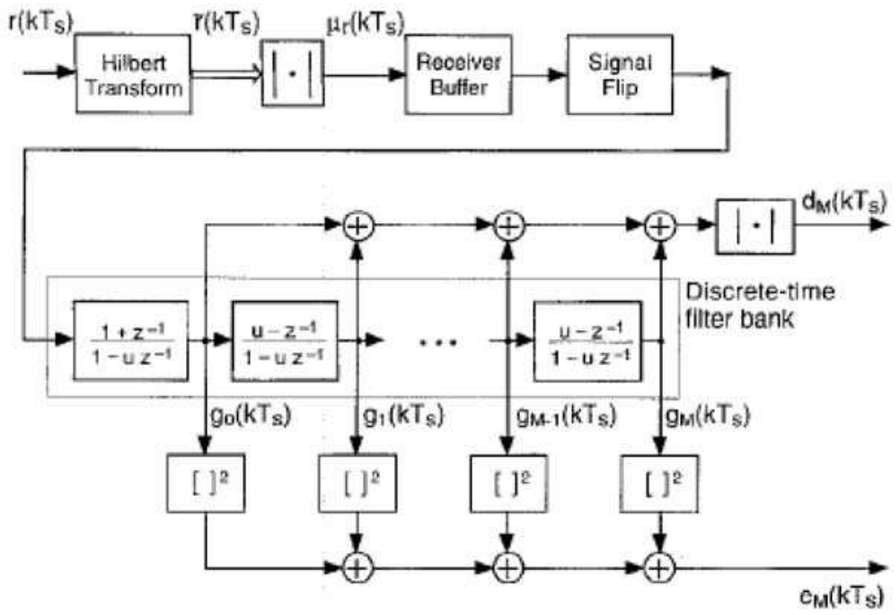

Fig. 6. Block diagram of the correlation receiver.

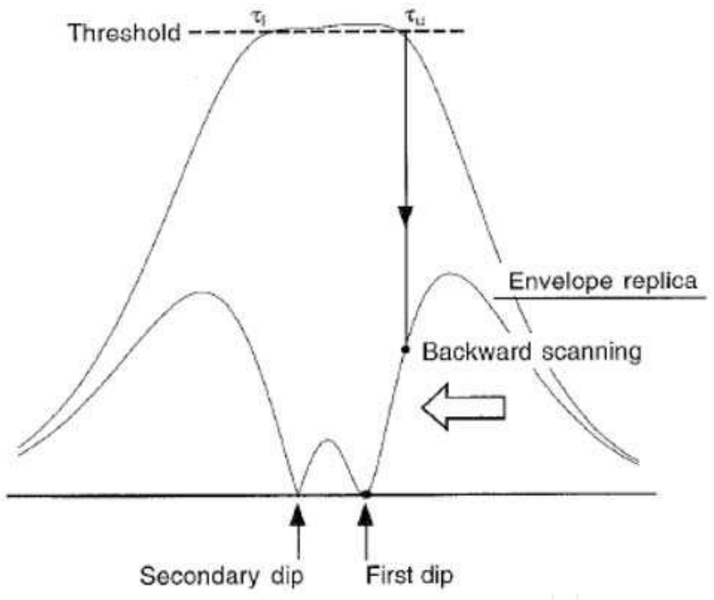

Fig. 7. Explanation of the proposed TOF algorithm (constrained correlation receiver).

3. Measurement method based on discrete extended Kalman filter

3.1 Discrete extended Kalman filter

The Discrete Kalman Filter (DKF) is generally adopted to estimate the state of a linear stochastic process. It uses a kind of feedback control based on measurement results of quantities that are linear functions of the state [9]. More specifically, the filter estimates the process state at a given time instant, and then obtains feedback by incorporating a new measurement result into the *a-priori* estimate in order to gain an improved *a-posteriori* estimate.

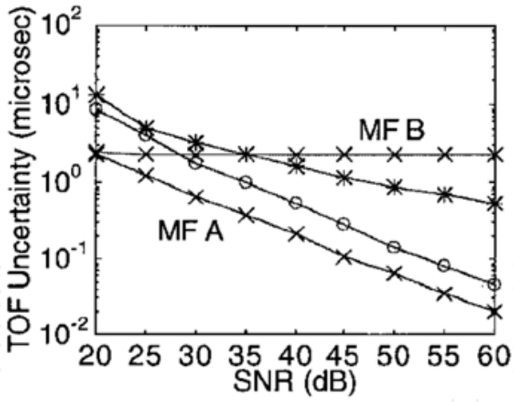

Fig. 8. - TOF estimation accuracy for *M*=4. MFA stands for unbiased cross correlation estimator, MFB is the biased version, symbol o indicate Constrained correlation receiver, and * identify unconstrained correlation receiver.

In the presence of a non-linear process, the DKF can still be adopted, provided that suitable linearization techniques are applied. Non-linear behaviors should affect the process through either dynamics or measurement equations. In the absence of control inputs, the evolution of a generic, discrete-time, non-linear process can be analyzed through the following non-linear equation system:

$$\begin{cases} x_k = f(x_{k-1}, k-1) + w_{k-1} \\ z_k = h(x_k, k) + v_k \end{cases} \tag{18}$$

where x_k is the current *n*-dimensional vector of the process state, z_k is the *m*-dimensional vector of current measurement results, *f* and *h* are known functions; $w_k \sim N(0,Q_k)$ and $v_k \sim N(0,R_k)$ are uncorrelated, noisy, Gaussian sequences [7].

Two linearization techniques are available in the literature: *discrete linearized Kalman filter* (DLKF) and *discrete extended Kalman filter* (DEKF). Both of them provides for linear approximation of the effect of small perturbation from a "nominal" value in the state of the non-linear system. DLKF is tailored to applications, such as guidance and control, in which the nominal values of the state variables are fairly well known beforehand. Thus, the estimation problem can effectively be linearized around the nominal trajectory (i.e. the sequence of nominal state vectors). When the process under analysis exhibits hard non-linear behavior, the deviation value of the actual trajectory from the nominal one usually tends to increase with time. In such cases, the higher-order approximation terms cannot be neglected, preventing DLKF to be extensively used.

DEKF gives a simple but effective remedy for this problem; the nominal trajectory is defined "on the fly" as the current best estimate of the actual trajectory. According to the DEKF theory, the actual state vector may be written as:

$$x_k = x_k^N + \delta x_k \tag{19}$$

$x_k^N = \hat{x}_{k-1}^+$ is the nominal trajectory assumed equal to the *a-posteriori* estimate of the state vector obtained at the previous step. If the perturbation, δx_k , has small value, *f* and *h* functions can be approximated through their first-order, Taylor's series expansions with

respect to x. With this assumption, the evolution of the process may be analyzed through the following implementation equations:

$$\begin{aligned} \hat{x}_k^- &= f(\hat{x}_{k-1}^+, k-1) + \Phi_{k-1}\delta x_{k-1} \\ \hat{P}_k^- &= \Phi_{k-1}\hat{P}_{k-1}^+\Phi_{k-1}^T + Q_k \\ \hat{z}_k^- &= h(\hat{x}_k^-, k) + \mathrm{H}_k\delta x_k \end{aligned} \tag{20}$$

where $\Phi_k = \left.\frac{\partial f(x,k)}{\partial x}\right|_{x=\hat{x}_{k-1}^+}$ is the state transition matrix and $\mathrm{H}_k = \left.\frac{\partial h(x,k)}{\partial x}\right|_{x=\hat{x}_k^-}$ is the measurement sensitivity matrix; $\hat{x}_k^-$, P_k^- and $\hat{z}_k^-$ stands respectively for *a-priori* (predicted) estimate of state vector, error covariance matrix and measurement results.
The resulting discrete-time update equations are

$$\begin{aligned} \hat{x}_k^+ &= \hat{x}_k^- + \overline{K}_k\left(z_k - \hat{z}_k^-\right) \\ \hat{P}_k^+ &= \left(I - \overline{K}_k\mathrm{H}_k\right)\hat{P}_k^- \end{aligned} \tag{21}$$

where $\hat{x}_k^+$ and $\hat{P}_k^+$ are *a-posteriori* (corrected) estimates, and $\overline{K}_k = \hat{P}_k^-\mathrm{H}_k^T\left(\mathrm{H}_k\hat{P}_k^-\mathrm{H}_k^T + R_k\right)^{-1}$ is the Kalman gain. Once evaluated the expression (21) the filter is ready to execute another recursive loop.
In recent scientific works [10],[11], the DEKF has been used to improve the accuracy of ultrasonic-based location systems of robots. In particular, TOF data provided by several ultrasonic sensors and collected as temporal readings are properly fused thanks to the exploitation of some nice properties of the DEKF.
In the following [12],[13], the DEKF is, instead, proposed as an original tool to jointly determine the TOF and shape parameters (A_0, α, and T) characterizing an ultrasonic echo envelope modeled according to:

$$A(t) = A_0\left(\frac{t-\tau}{T}\right)^{\alpha}\exp\left(\frac{t-\tau}{T}\right) \tag{22}$$

Details concerning the suggested use of the DEKF and its action in the framework of the adopted measurement procedure are given below.

3.2 Application of DEKF to ultrasonic echoes

The key idea underlying the proposed use of the DEKF consists of defining the state vector $x=[A_0, \alpha, T, \tau]$ through the considered parameters of the ultrasonic echo envelope. This way, the generic equations system (18) is simplified, since these parameters can be considered constant once the ultrasonic echo has been acquired. Moreover, once $\hat{x}_k^+$ is determined, it is taken as the nominal trajectory for the subsequent recursive loop. With the last assumptions, the perturbation δx_k of the expression (19) is null for each k, while the state transition matrix, Φ_k, reduces itself to the unity matrix, I. Finally, since the state has no superimposed noise, Q_k matrix is always null. The time update equations (21) take so the form:

$$\hat{x}_k^- = \hat{x}_{k-1}^+ \qquad \hat{P}_k^- = \hat{P}_{k-1}^+ \tag{23}$$

With regard to the matrix R_k, it has 1x1 dimension, and its element is the variance of the superimposed measurement noise.
The basic loop of the recursive procedure to evaluate the discrete-time Kalman estimator of the state vector x_k is as follows (Fig.9).

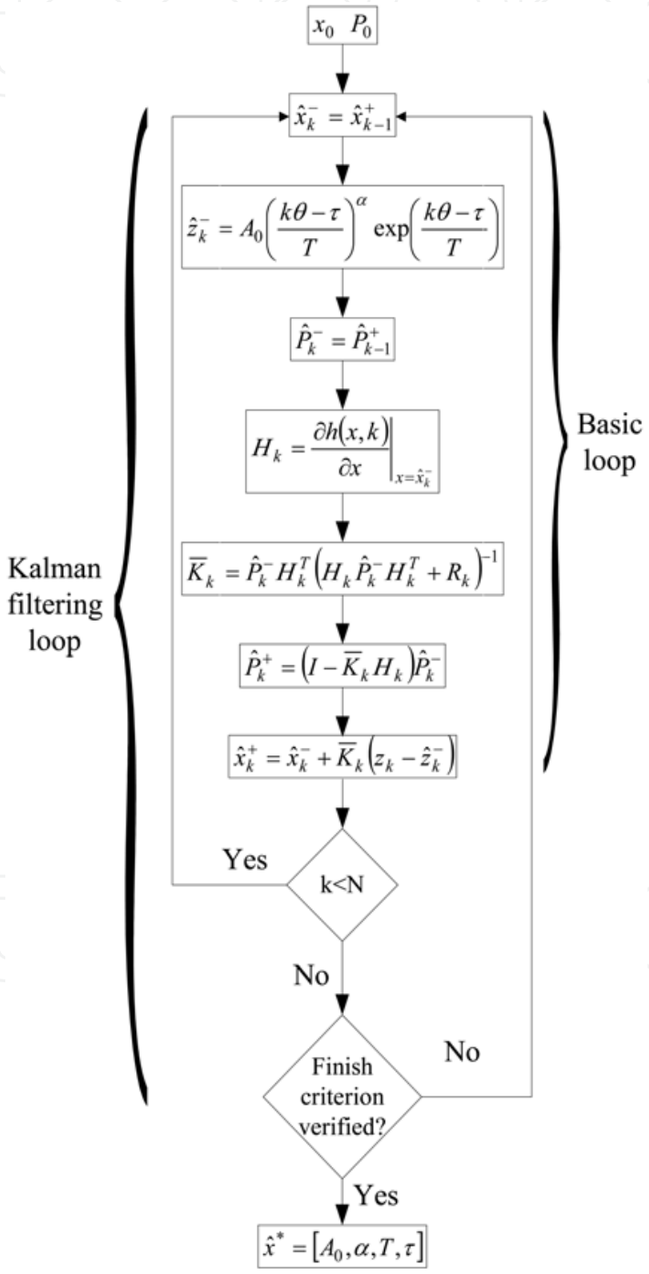

Fig. 9. - Flow diagram of the recursive procedure that specifies the application of DEKF to ultrasonic echoes; N is the number of samples included in the observation interval.

1. *A-priori* estimation of the state vector:

$$\hat{x}_k^- = \hat{x}_{k-1}^+$$

2. *A-priori* estimation of the measurement result through the equation (22):

$$\hat{z}_k^- = A_0\left(\frac{k\theta-\tau}{T}\right)^{\alpha}\exp\left(\frac{k\theta-\tau}{T}\right)$$

where θ is the sampling period, and A_0, α, T, and τ represent the values of the parameters obtained at the previous step.

3. *A-priori* estimation of the error covariance matrix:

$$\hat{P}_k^- = \hat{P}_{k-1}^+$$

the matrix has 4x4 dimension.

4. Evaluation of the measurement sensitivity matrix:

$$\mathrm{H}_k = \left.\frac{\partial h(x,k)}{\partial x}\right|_{x=\hat{x}_k^-}$$

the matrix has 4x1 dimension.

5. Calculation of the Kalman gain:

$$\overline{K}_k = \hat{P}_k^- \mathrm{H}_k^T\left(\mathrm{H}_k\hat{P}_k^-\mathrm{H}_k^T + R_k\right)^{-1}$$

6. *A-posteriori* estimation of the state vector conditioned on the current measurement result:

$$\hat{x}_k^+ = \hat{x}_k^- + \overline{K}_k\left(z_k - \hat{z}_k^-\right)$$

7. *A-posteriori* estimation of the error covariance matrix:

$$\hat{P}_k^+ = \left(I - \overline{K}_k H_k\right)\hat{P}_k^-$$

The basic loop is iterated all along the observation interval including the echo envelope of interest. Once the iteration is over (i.e. the whole observation interval has been examined), a single Kalman filtering loop of the recursive procedure is completed (Fig.9). The recursive procedure stops when a suitable finish condition is met; the elements of the state vector $\hat{x}^*$ corresponding to the last state estimate give the desired parameters of the ultrasonic echo envelope.

3.3 Initial conditions and recursion finish criterion

The described recursive procedure can be executed once *(i)* the starting estimates of the state vector and error covariance matrix, referred to respectively as x_0 and P_0, *(ii)* the experimental variance of measurement noise, R_0, and *(iii)* the recursion finish criterion are available.

With regard to *(i)*, some preliminary considerations are needed. Specifically, the generic element x_i is modeled as random variate, and it can take values in a specific interval $[x_{i1}, x_{i2}]$.

For each parameter, in fact, a suitable range of values has to be fixed according both to their typical interval of variation [14] and user's knowledge and experience. In particular:

1. with regard to A_0, typical values of the amplitude of received echoes should be considered;
2. concerning α, typical slopes that the rising edge of received echoes exhibits in proximity to the onset should be accounted for;
3. referring to T, typical durations of the ultrasonic transmission burst should be enlisted;
4. as for TOF, the related interval is automatically established after the signal preprocessing step of the measurement procedure, details of which are given below.

Assuming a rectangular probability density function for each element x_i, the starting estimates of the element and its variance are given by:

$$\hat{x}_{i0} = \frac{1}{2}(x_{i2} + x_{i1})$$
$$\sigma_{i0}^2 = \frac{1}{12}(x_{i2} - x_{i1})^2 \tag{24}$$

This way, P_0 is a diagonal matrix, the elements of which correspond to the variances of the starting estimates.

As for *(ii)*, the variance of the noise floor of the adopted data acquisition system should be measured.

Concerning *(iii)*, it is worth noting that, if the problem is well-conditioned, a better state vector estimate is achieved for each execution of the Kalman filtering loop. A suitable finish criterion is thus needed. At this aim, the value of the modulus of the difference between the state vector estimates provided by two consecutive Kalman filtering loops is compared to a proper threshold value (empirical tests suggest the value of $1 \cdot 10^{-4}$). If the difference is lower than the threshold, the recursive procedure stops, and the best estimate of the four parameters of the echo envelope is delivered; otherwise, a new Kalman filtering loop is executed.

3.4 Measurement procedure

The fundamental steps of the DEKF-based measurement procedure are described with reference to a clarifying example.

- *Digitization*

The ultrasonic signal is at first digitized by means of a data acquisition system, the characteristics of which, in terms of sample rate and memory depth, have to be chosen appropriately. Specifically, the adopted sample rate, f_c, has to satisfy the Nyquist lower bound, and, along with the memory depth, has to grant an appropriate observation interval according to the desired TOF measurement range.

Fig.10 shows an ultrasonic signal characterized by a center frequency of 43.8 kHz and digitized at sample rate of 250 kS/s; multiple echoes can be noted.

- *Signal pre-processing*

As already stated, the proposed recursive procedure is expected to work on the envelope of the ultrasonic echo of interest. After digitization, pre-processing operations are, thus, needed. In particular, the portion of the digitized signal, accounting for the ultrasonic transmission burst, is firstly cut; in the application example the removed portion covers 2

ms. The envelope of the remaining signal is, then, given by the modulus of its analytical version, attained through an ordinary Hilbert transform (Fig.11). If the transmitted ultrasonic burst undergoes multiple reflections, more than one echo is present in the obtained envelope. As a consequence, the echo of interest (generally, the main one) is, finally, isolated through the location of the maximum of the envelope and the selection of the portion, including this maximum, whose values are not buried in the noise floor (Fig.12).

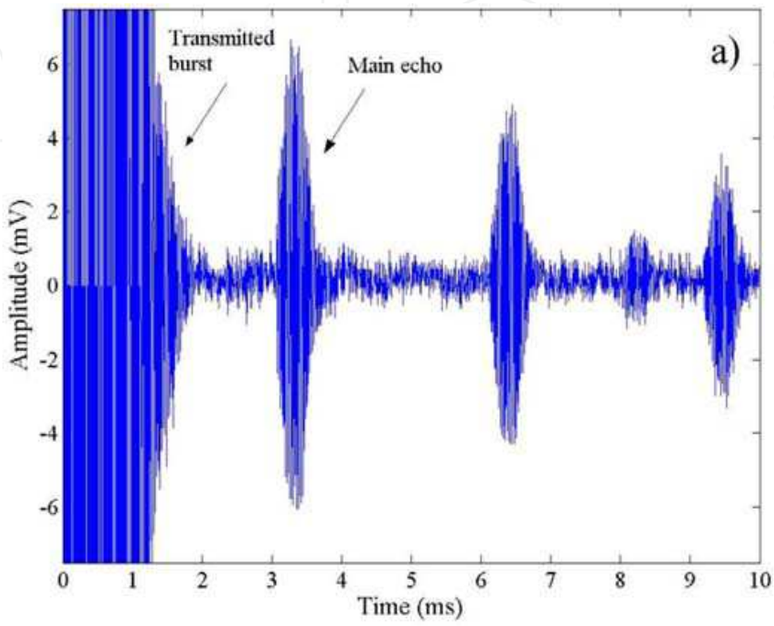

Fig. 10. Fundamental steps of the measurement procedure. a) Original ultrasonic signal digitized at a sample rate of 250 kS/s.

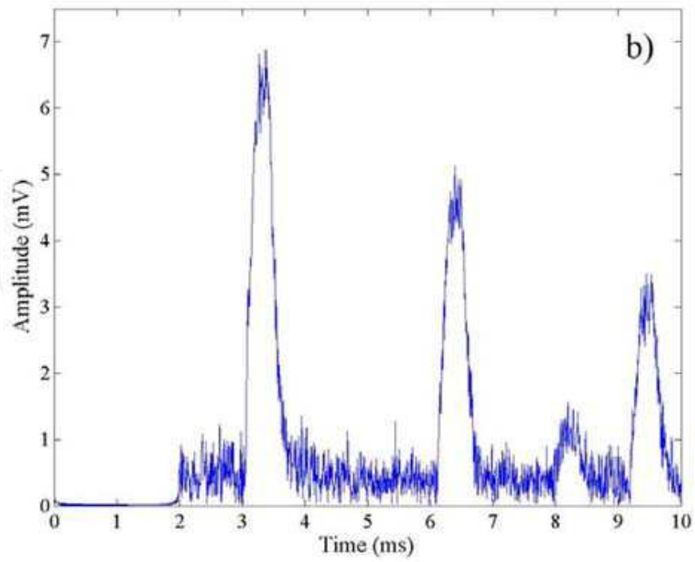

Fig. 11. Fundamental steps of the measurement procedure. b) envelope provided by the Hilbert transform: its null portion accounts for the cut that the original digitized signal has undergone;

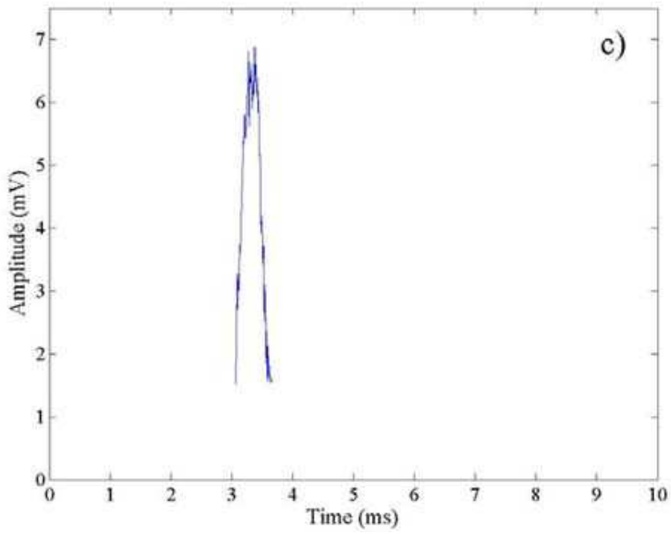

Fig. 12. Fundamental steps of the measurement procedure. c) location and isolation results of the echo of interest.

- *TOF and shape parameters estimation*

Before applying the proposed recursive procedure, the variation interval, [x_{i1}, x_{i2}], of the TOF has to be assigned in order to fix the starting estimates of the TOF itself and its variance, according to what stated above. The upper bound, x_{i2}, is given by the time instant characterizing the first value of the echo of interest obtained at the end of the previous step; in the considered example it is equal to 3.068 ms. The lower bound, x_{i1}, is then gained by subtracting from x_{i1} a suitable number of sampling intervals; the experimental tests have shown that 50 sampling intervals are appropriate to the purpose.

After fixing the initial estimates of the state vector and error covariance matrix, the recursive procedure can run, thus giving, at the end, the wanted values of the TOF and shape parameters of the echo of interest.

Concerning the application example, Fig.13 shows the superposition of the envelope reconstructed by substituting in (22) the values of A_0, α, T, and τ provided by the proposed method to the original digitized signal; it can be appreciated how well the obtained envelope fits the experimental data.

3.5 Performance assessment

To assess the performance of the proposed method, a number of tests on simulated and actual ultrasonic signals have been carried out.

Tests conducted on simulated signals

Ultrasonic echo envelopes have been synthesized numerically in the hypothesis of a sample rate equal to 250 kS/s. The values of the shape parameters are very similar to those peculiar to the actual signals involved in the successive experimental tests. The obtained envelopes have then modulated a sinusoidal carrier, the frequency of which matches that of the ultrasonic transmitter (43.8 kHz) adopted in the experimental tests. The resulting signals have finally been corrupted by additive, white, Gaussian noise.

After fixing the interval of variation of the shape parameters, [3 mV, 30 mV] for A_0, [1, 3] for α, and [100 μs, 150 μs] for T, several tests have been conducted for different values both of

TOF, in order to account for various distances or levels (within 35-175 cm) to be measured, and signal-tonoise ratio, SNR (within 20-60 dB), in order to simulate diverse noise conditions of the measurement chain. For the sake of clarity, Fig.14 shows the superposition of an envelope reconstructed by the proposed method to the related, original signal, characterized by a TOF of 4.5 ms.

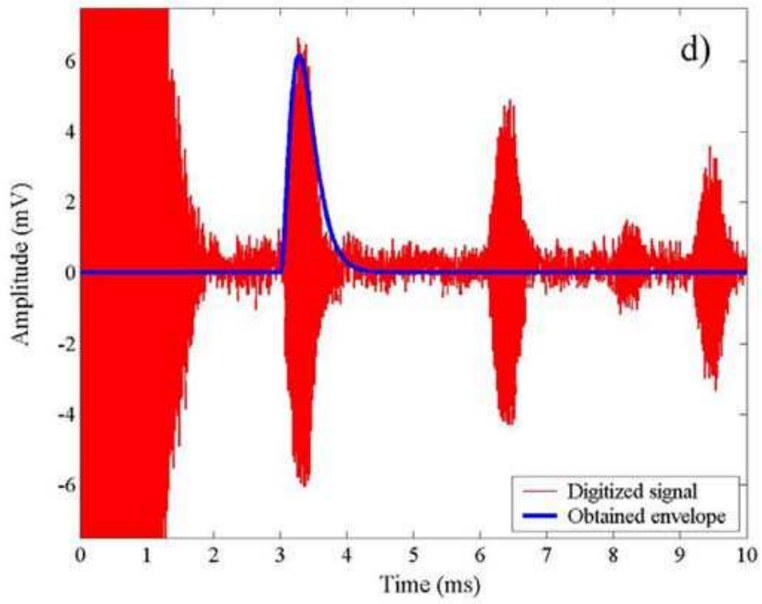

Fig. 13. Fundamental steps of the measurement procedure. d) superposition of the envelope reconstructed by the proposed method to the original digitized signal.

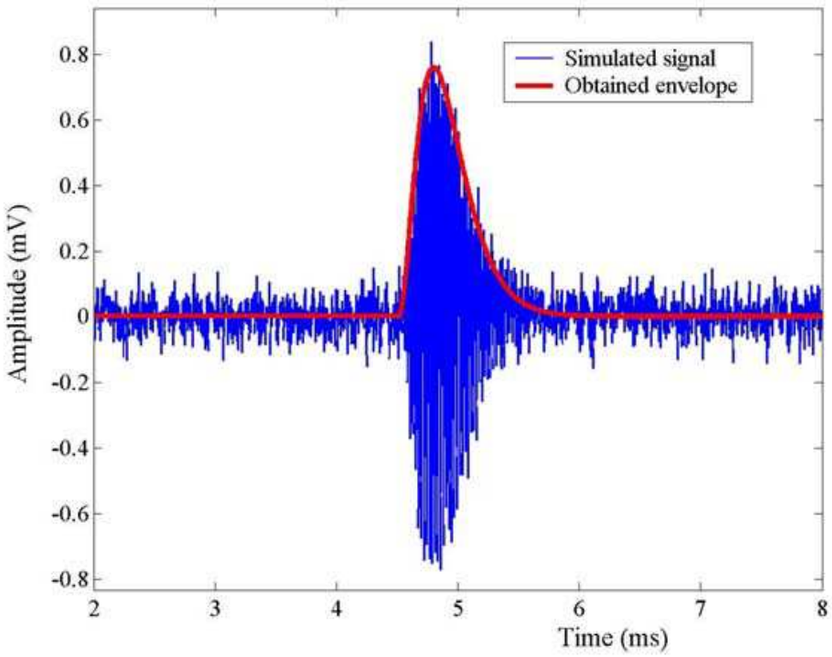

Fig. 14. Superposition of an envelope reconstructed by the proposed method to the related, original signal, characterized by a TOF of 4.5 ms.

For each couple of values of TOF and SNR, about 100 ultrasonic signals have been analyzed. From the obtained results, bias and experimental standard deviation, σ, on TOF estimates have been evaluated. In particular, the bias is given by the difference between the mean value of the TOF estimates and the imposed one. Values of bias and σ lower respectively than 2.8 μs and 5.3 μs have always been experienced. In the presence of a temperature equal to 24°C, these values correspond to a bias and experimental standard deviation on distance estimates equal respectively to 970 μm and 1834 μm. Moreover, a proper figure of merit, *MSE*, which quantifies the performance exhibited by the proposed method in reconstructing ultrasonic echo envelopes, has also been evaluated. *MSE* is given by

$$MSE = 10\log_{10}\frac{\sum_{k=1}^{N}(Ar_k - A_k)^2}{\sum_{k=1}^{N}A_k{}^2} \tag{25}$$

where N is the number of samples included the observation interval; A_k and Ar_k stands for the amplitude of respectively reference and reconstructed echo at the time instant $k\theta$. Values of *MSE* lower than -20 dB have been achieved also in critical measurement conditions (very low SNR values and high degree of echo distortion).

Tests conducted on actual signals

Some experiments have been conducted through a suitable measurement station capable of generating and acquiring ultrasonic signals. It has included (i) a processing and control unit (PCU), namely a personal computer, (ii) an ultrasonic transmitter/receiver (UT), *Polaroid 9000 Series,* (10°x40° beam angle, 43.8 kHz carrier frequency), (iii) a data acquisition system (DAQ), *Tektronix 210*, (8-bit resolution, 60-MHz bandwidth, 1-GS/s maximum sample rate) and (iv) a set of reference distances realized by a calibrated sliding plane. The PCU and the DAQ have been linked together by means of an IEEE-488 interface bus.

The PCU has driven the UT (acting as transmitter) with a rectangular burst, consisting of 16 cycles, through the line-0 of its parallel port. At the same time, it has generated a synchronization pulse on the line-1 of the same parallel port. The signal coming from the UT, accounting both for the transmitted ultrasonic pulse and received echo, has been digitized by the DAQ, and stored in a record covering a time-window of 10 ms (2500 samples). The DAQ has exhibited a vertical scale of 2 mV/div, and it has externally been triggered through the synchronization pulse generated by the PCU. To accurately estimate the propagation velocity, the temperature of the coupling medium, namely the air, has duly been checked throughout the measurement process; a standard RTD probe has been adopted.

In the following sub-sections, results are presented in terms of bias, δ, and experimental standard deviation, σ, obtained by statistically processing the values provided by about one hundred acquisitions for each value of distance or tilt angle.

- *Tests conducted in free-space propagation*.

A number of experimental tests in free-space propagation have preliminarily been conducted to assess the performance of the method in the best measurement conditions (i.e.

perfect orthogonality between the source and target, and measurement environment without acoustic interferences). The ultrasonic source has been mounted on a sliding plane, while the target has been realized by means of a fixed metallic surface. The distance between the source and target has been measured with a proper reference (Fig.15).

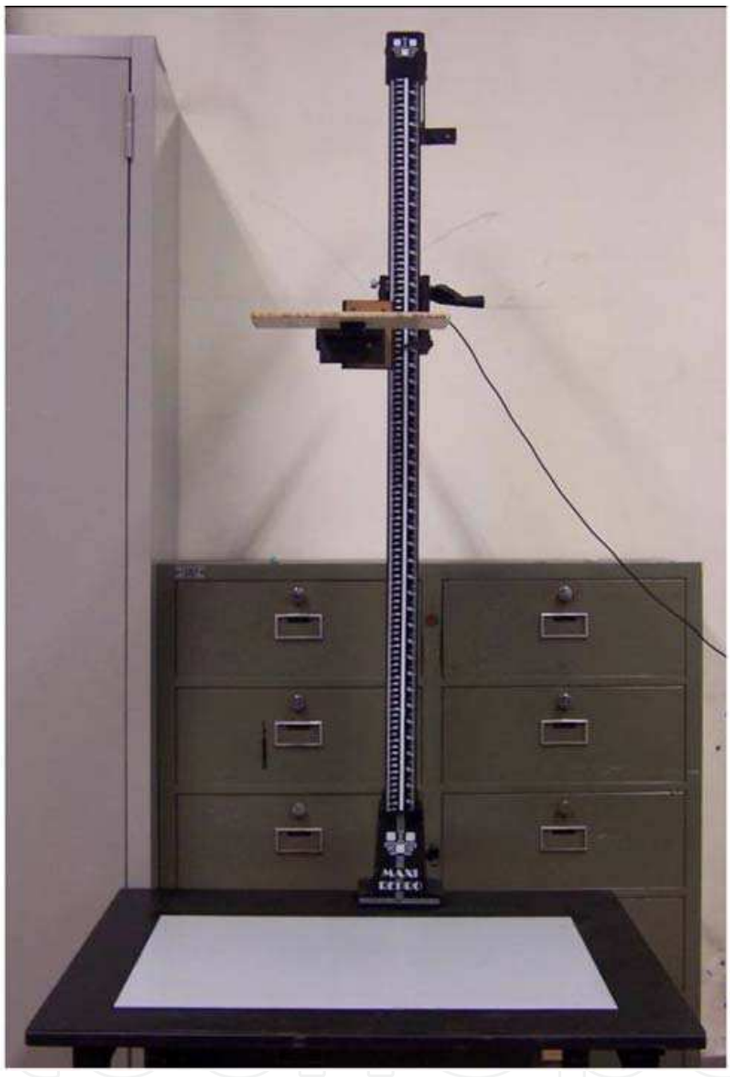

Fig. 15. Experimental apparatus adopted in tests in free-space propagation.

The performance of the method has been investigated upon the distance's varying in the interval equal to 400-1000 mm. The obtained results, both expressed in percentage relative terms, are given in Fig.16; values of δ and σ respectively lower than 0.2% and 0.4% have always been experienced.

- *Tests conducted in closed-tank configuration*

This kind of tests has been conducted to assess the robustness of the proposed method in the presence of multiple echoes or reverberation. At this aim, the worst measurement configuration has been adopted: the ultrasonic source has been positioned on the axis of a

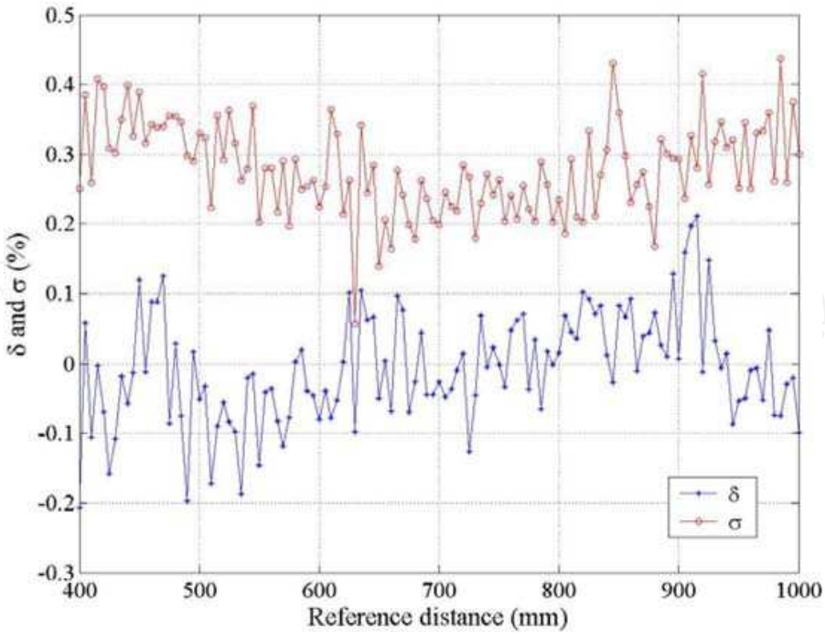

Fig. 16. Values of δ and σ, both expressed in relative percentage terms, obtained in tests in free-space propagation.

Fig. 17. Experimental apparutus adopted in tests in closed-tank configuration.

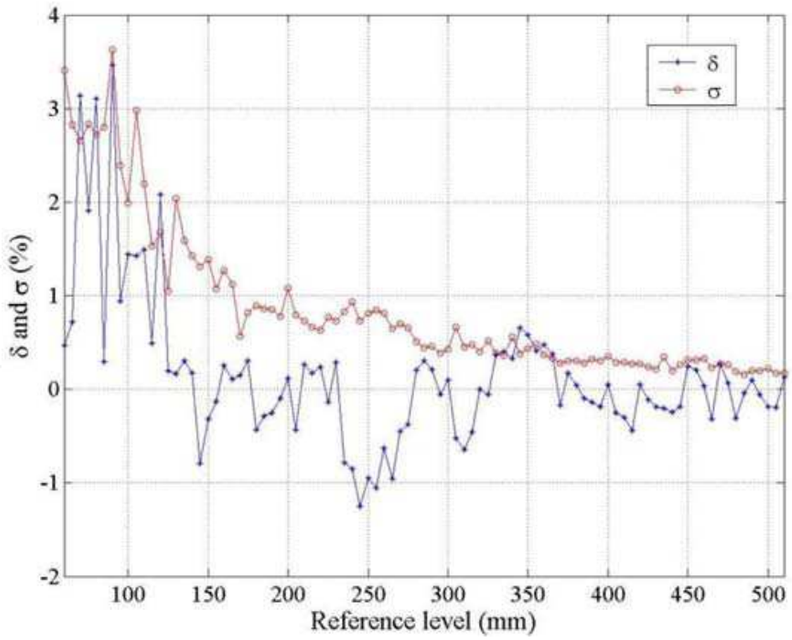

Fig. 18. Values of δ and σ, both expressed in relative percentage terms, obtained in tests in closed tank configuration.

Fig. 19. Experimental apparatus adopted in tests in misalignment conditions.

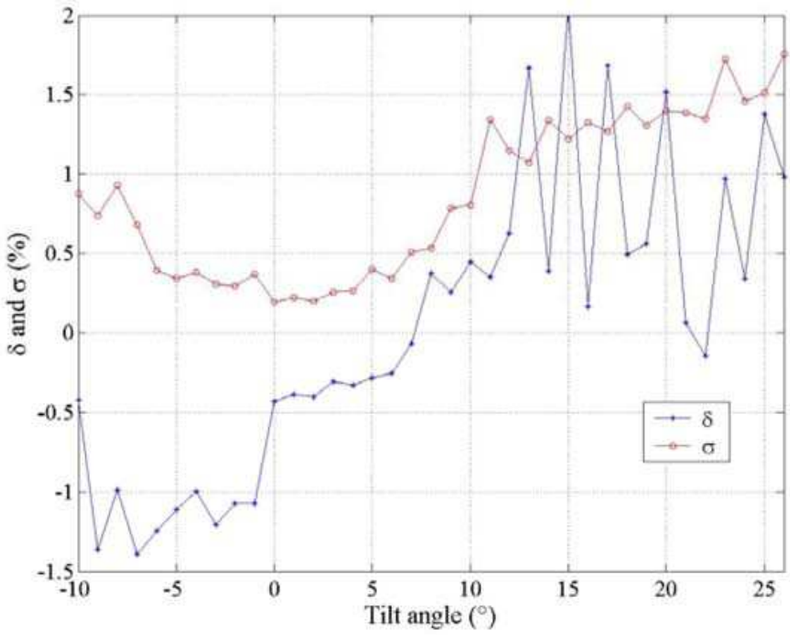

Fig. 20. Values of δ and σ, both expressed in relative percentage terms, obtained in tests in misalignment condition for a reference distance of 41 cm.

cylindrical tank (Fig.17). The level of the fluid is then calculated as difference between the measured distance of liquid-air interface and the known distance of tank bottom.

The performance of the method has been investigated upon the level's varying in the interval equal to 60-510 mm. The obtained results, both expressed in percentage relative terms, are given in Fig.18; values of δ and σ similar to those granted in free-space propagation tests have been experienced, except for the lowest levels.

- *Tests conducted in misalignment conditions*

The effect on measurement results of misalignment between the reflecting plane and ultrasonic source has then been investigated. The adopted apparatus is represented in Fig.19. It consists of the same sliding plane of the free-space propagation test and a target plane that rotates around its own axes; the angular position of the rotating plane has been measured through a reference goniometer.

It has been experienced, as expected, that the amplitude of the received echo was decreased upon the increasing of the tilt angle or distance. As an example, results, both expressed in percentage relative terms, obtained for a reference distance of 41 cm are given in Fig.20; similar results have been obtained for the other examined distances.

Values of δ and σ similar to those granted in free-space propagation tests have been experienced in a wide range of examined angular positions of the target plane.

4. References

[1] P. Kleinschmidt and V. Magori, Ultrasonic robotic-sensors for exact short range distance measurement and object identification, *Ultrasonics Symp. Proc*, IEEE, 1985, Vol.1, pp.457-462.

[2] D. Marioli, E. Sardini and A. Taroni, Ultrasonic distance measurement for linear and angular position control, IEEE Trans. lustrum. Meas. Vol.37, N.4, December 1988, pp.578-581.
[3] C. Lougblin, Ultrasonic measurement: keeping your distance, *Sensor Rev*., April 1989, pp.85- 89.
[4] G. Hayward and Y. Gorfu, A digital hardware correlation system for fast ultrasonic data acquisition in peak power limited applications, *IEEE Trans. Ultrason. Ferroelec. Freq. Control*, Vol.35, N.6, November 1988, pp. 800-808.
[5] LM 1812 Ultrasonic Transceiver, National Semiconductor Special Purpose Linear Devices Databook, 1989, pp. 9/77-9/84.
[6] Murata ultrasonic sensors, Murata Products 1991, 1991, p. 77.
[7] Honeywell ultrasonic distance sensors Series 942, Honeywell Data Sheet El 01, 1989.
[8] S. Kocis, Z. Figura, Ultrasonic Measurements and Technologies, Chapman and Hall, London, 1996.
[9] D. Marioli, C. Narduzzi, C. Offelli, D. Petri, E. Sardini, A. Taroni, Digital time-of-flight measurement for ultrasonic sensors, IEEE Trans, lustrum. Meas., Vol.41, N.1, February 1992, pp.93-97.
[10] F.E. Gueuning, M. Varlan, C.E. Eugene, P. Dupuis, Accurate Distance Measurement by an Autonomous Ultrasonic System Combining Time-of-Flight and Phase-Shift Methods, IEEE Trans. on Instr. and Meas., Vol.46, N.6, December 1997, pp.1236-1241.
[11] P. Kleinschmidt and V. Magori, "Ultrasonic remote sensors for noncontact object detection," Siemens Forsch. Entwickl.ber., vol. 10, no. 2, pp. 110-118, 1981.
[12] H. Peremans, K. Audenaert, and J. Van Campenhout, "A high-resolution sensor based on triaural perception," IEEE Trans. Robot. Automat, vol. 9, no. 1, pp. 36-48, 1993.
[13] N. J. Nilsson, "On the optimum range resolution of radar signals in noise," IRE Trans. Inform. Theory, vol. 32, no. 7, pp. 245— 253, 1961.
[14] H. Eriksson, P. O. Borjesson, P. Odling and N.-G. Holmer, "A robust correlation receiver for distance estimation," IEEE Trans. Ultrason., Ferroelect., Freq. Contr., vol. 41, no. 5, pp. 596— 603, 1994.
[15] P. Eykhoff, System Identification. New York: Wiley, 1974.
[16] Y. W. Lee, Statistical Theory of Communication. New York: Wiley, 1960.
[17] T. Oliveira e Silva, "On the determination of the optimal pole position of Laguerre filters," IEEE Trans. Signal Processing, vol. 43, no. 9, pp. 2079-2087, 1995.
[18] A. C. Den Brinker, "Adaptive modified Laguerre filters," Signal Process., vol. 31, pp. 69-79, 1993.
[19] P. M. Gammell, "Improved ultrasonic detection using the analytic signal magnitude," Ultrasonics, vol. 19, no. 2, pp. 73-76, 1981.
[20] A. M. Sabatini, "Correlation receivers using Laguerre filter banks for modelling narrowband ultrasonic echoes and estimating their time-of-flights," IEEE Trans. on Ultr., Ferr. and Freq. Contr., vol.44, No.6, pp.1253–1263, Nov. 1997.
[21] M.S.Grewal, A.P.Andrews, Kalman filtering. Theory and practice, Englewood Cliffs, NJ, Prentice Hall, 1993.

[22] C.Tsai, "A Localization System of a Mobile Robot by Fusing Dead-Reckoning and Ultrasonic Measurements," IEEE Trans. on Instr. and Meas., vol.45, No.5, pp.1399-1404, October 1998.

[23] P.Ramuhalli, J.Kim, L.Udpa, S.S.Udpa, "Multichannel signal processing methods for ultrasonic nondestructive evaluation," Proc. of Sensor Array and Multichannel Signal Processing Workshop, pp.229 233, Aug. 2002.

Kalman Filter Recent Advances and Applications

Edited by Victor M. Moreno and Alberto Pigazo

ISBN 978-953-307-000-1
Hard cover, 584 pages
Publisher InTech
Published online 01, April, 2009
Published in print edition April, 2009

The aim of this book is to provide an overview of recent developments in Kalman filter theory and their applications in engineering and scientific fields. The book is divided into 24 chapters and organized in five blocks corresponding to recent advances in Kalman filtering theory, applications in medical and biological sciences, tracking and positioning systems, electrical engineering and, finally, industrial processes and communication networks.

InTech Europe
University Campus STeP Ri
Slavka Krautzeka 83/A
51000 Rijeka, Croatia
Phone: +385 (51) 770 447
Fax: +385 (51) 686 166
www.intechopen.com

InTech China
Unit 405, Office Block, Hotel Equatorial Shanghai
No.65, Yan An Road (West), Shanghai, 200040, China
中国上海市延安西路65号上海国际贵都大饭店办公楼405单元
Phone: +86-21-62489820
Fax: +86-21-62489821

IntechOpen